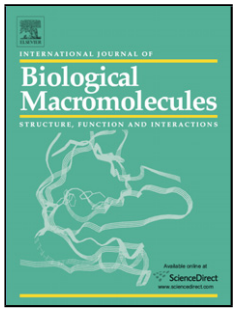

Title: Chitosan nanoparticles enhances the anti-quorum sensing activity of kaempferol

Author: Sedef Ilk Necdet Sağlam Mustafa Özgen Feza Korkusuz

PII: S0141-8130(16)32087-6
DOI: http://dx.doi.org/doi:10.1016/j.ijbiomac.2016.10.068
Reference: BIOMAC 6648

To appear in: *International Journal of Biological Macromolecules*

Received date: 6-6-2016
Revised date: 16-10-2016
Accepted date: 20-10-2016

Please cite this article as: Sedef Ilk, Necdet Sağlam, Mustafa Özgen, Feza Korkusuz, Chitosan nanoparticles enhances the anti-quorum sensing activity of kaempferol, International Journal of Biological Macromolecules http://dx.doi.org/10.1016/j.ijbiomac.2016.10.068

Chitosan nanoparticles enhances the anti-quorum sensing activity of kaempferol

Sedef Ilk[a, *], Necdet Sağlam[b], Mustafa Özgen[c], Feza Korkusuz[d]

[a]Faculty of Ayhan Şahenk Agricultural Sciences and Technologies, Nigde University, 51240 Nigde, Turkey

[b]Department of Nanotechnology and Nanomedicine, The Institute of Science and Engineering, Hacettepe University, Beytepe, 06800 Ankara, Turkey

[c]Department of Plant Production and Technologies, Faculty of Ayhan Şahenk Agricultural Sciences and Technologies, Nigde University, 51240 Nigde, Turkey

[d]Department of Sports Medicine, Faculty of Medicine, Hacettepe University, Beytepe, 06800 Ankara, Turkey

*Corresponding author: Ayhan Sahenk Agricultural Sciences and Technologies Faculty, Nigde University, 51240 Nigde,Turkey.

Tel: +90 388 2254449 (office); fax: +90 388 2254440

E-mail:sedefilk@nigde.edu.tr

Highlights

- Kaempferol loaded chitosan/TPP nanoparticles were prepared based on the electrostatic self-assembly method.
- Novel kaempferol loaded chitosan/TPP nanoparticles were confirmed by SEM, FTIR, NMR, DSC and XRD analysis.
- QS inhibition of kaempferol loaded chitosan/TPP nanoparticles was measured in violacein pigment producing using *Chromobacterium violaceum CV026* strain.
- Kaempferol loaded chitosan nanoparticles can inhibit QS related processes opens up an exciting new strategy for antimicrobial method as stable QS-based anti-biofilm agents.

A B S T R A C T

Quorum sensing (QS) is a cell density dependent expression of species in bacteria mediated by compounds called autoinducers (AI). Several processes responsible for successful establishment of bacterial infection are mediated by QS. Inhibition of QS is therefore being considered as a new target for antimicrobial chemotherapy. Flavonoid compounds are strong antioxidant and antimicrobial agents but their applications are limited due to their poor dissolution and bioavailability. Our objective was to investigate the effect of kaempferol loaded chitosan nanoparticles on modulating QS mediated by AI in model bioassay test systems. For this purpose, kaempferol loaded nanoparticles were synthesized and characterized in terms of hydrodynamic diameter, hydrogen bonding, amorphous transformation and antioxidant activity. QS inhibition in time dependent manner of nanoparticles was measured in violacein pigment producing using the biosensor strain *Chromobacterium violaceum CV026* mediated by AI known as acylated homoserine lactone (AHL). Our results indicated that the average kaempferol loaded chitosan/TPP nanoparticle

size and zeta potential were 192.27±13.6 nm and + 35 mV, respectively. The loading and encapsulation efficiency of kaempferol into chitosan/TPP nanoparticles presented higher values between 78-93%. Kaempferol loaded chitosan/TPP nanoparticle during the 30 storage days significantly inhibited the production of violacein pigment in *Chromobacterium violaceum CV026*. The observation that kaempferol encapsulated chitosan nanoparticles can inhibit QS related processes opens up an exciting new strategy for antimicrobial chemotherapy as stable QS-based anti-biofilm agents.

Keywords: Anti-Quorum Sensing, Biofilm Formation, Kaempferol, Chitosan Nanoparticle, *Chromobacterium violaceum.*

1. Introduction

Many bacterial species communicate with each other in a population-dependent mechanism to regulate their physiological functions. This mechanism is called as quorum sensing (QS) which is mediated through the release of diffusible and small signaling molecules called as autoinducers [1]. QS is an important process involved in bacterial survival and infections, recent research has focused on the development of therapeutic agents which prevent or manage bacterial pathogenesis by inhibiting bacterial QS. The inhibition of QS offers an alternative to antibiotic mediated bactericidal approach and reduces the risk for development of resistance. Inhibition of bacterial QS by attenuating the signals can prevent the development of bacterial virulence and successful establishment of infections [2]. Natural compounds have earned more attention as a source of anti-QS compounds for the treatment of biofilms [3]. Many gram negative bacteria, including *Chromobacterium violaceum (C. violaceum)*, use N-acyl homoserine lactones (AHLs), signal molecules to monitor their own

population density. *C. violaceum* is commonly found in soil and water, particularly in the tropical and subtropical areas and produces violacein, a purple pigmented compound when N-hexanoylhomoserine lactone (C6-HSL) is present [4, 5]. *C. violaceum* CV026 is a mini-Tn5 mutant of *C. violaceum* which does not produce violacein unless it is supplied with C6-HSL. *C. violaceum CV026* lacks the autoinducer synthase CviI and thus requires exogenous C6-HSL for violacein formation, which is QS-mediated [6].

Flavonoid compounds have a significant effect in natural antimicrobial applications. Although kaempferol (KAE) has a wide range of health benefits including anti-inflammatory, anticancer and antioxidant advantages while its biological effects are limited due to low aqueous solubility. Previous studies have reported that limited water solubility and poor dissolution of flavonoids effected their chemical stability and bioavailability [7]. The use of nanoparticles can emerge to improve the solubility and bioavailability of KAE in a controlled manner through increased absorption and enhanced stability against free radicals during consumption and storage of food compounds [8]. Moreover, nanoparticles are suitable for efficient and sustainable delivery of active compounds and their large surface area enables rapid penetration of actives. Chitosan is a cationic and linear heteropolysaccharide composed of units of N-acetylglucosamine and glucosamine. It is linked by β-1,4 bonds and showed multiple properties such as biocompatibility, biodegradability, bioadhesion, absence of allergenicity and toxicity, anti-hypercholesterolemic, and antimicrobial activity. Therefore, chitosan has been presented as having potential for application in the industries of food, cosmetics, and pharmaceutics [9]. The aim of the present study is to develop a novel nanoparticle system (kaempferol loaded chitosan nanoparticle) to elucidate the anti-QS mechanism against reporter strain *Chromobacterium violaceum CV026.*

2. Materials and methods

2.1. Chemicals

Chitosan (75-85% deacetylated, low molecular weight), kaempferol (KAE, 99% purity), sodium tripolyphosphate (TPP), sodium hydroxide (NaOH), glacial acetic acid, phosphate buffer saline (PBS) tablets (pH: 7.4) and dimethylsulfoxide (DMSO) were purchased from Sigma-Aldrich. Luria-Bertani (LB) was supplied by LABM. Other chemicals and solvents were of analytical reagent grade.

2.2. Preparation of kaempferol-loaded chitosan/TPP nanoparticles

Kaempferol-loaded chitosan/TPP nanoparticles were prepared according to methods of Calvo et al. [10] and Fan et al. [11] with some modifications, based on the ionic gelation of chitosan with TPP anions. Chitosan (0.2 %, *w/v)* was dissolved in an aqueous solution of acetic acid (0.1 %, *v/v).* The pH of the chitosan solution was adjusted to 4.8 using aqueous NaOH solution (20 %, *w/v*). TPP (0.2 %, *w/v*) was dissolved in ultrapure water. Kaempferol solutions at concentration of 20, 30, 40, 60, 80 and 100 µg/mL were prepared in DMSO (10%, *v/v*). To prepare kaempferol loaded chitosan/TPP nanoparticles; into 10 mL of the preheated chitosan solution (60 °C for 10 min.), kaempferol solution was added under magnetic stirring. After that, 3.3 mL of 4 °C TPP solution was injected by dropwise (injection rate: 1 mL/min, syringe internal diameter: 0.38 mm) in chitosan/kaempferol solution at room temperature under magnetic stirring at 1000 rpm for 30 min. Opalescent suspension was formed spontaneously. The nanoparticles suspension was then centrifuged (12000 rpm, 30 min.) and washed with water to remove the unencapsulated compounds. After centrifugation, nanoparticle suspension was sonicated for 10 min. to avoid the aggregation of particles. The empty chitosan/TPP nanoparticles were synthesized with above described method using chitosan and TPP solution without kaempferol solution.

2.3. Determination of hydrodynamic diameter and zeta potential of the nanoparticles

The particle size, polydispersity index (PDI) and zeta potential of the kaempferol loaded chitosan nanoparticles were determined by dynamic light scattering (Zetasizer Nano ZS, Malvern Instruments, UK) at 25 °C. The nanoparticle solutions were analyzed in a folded capillary cell. All measurements were carried out in triplicate with three replications. The results were presented as mean ± standart deviation of the obtained values.

2.4. Determination of encapsulation efficiency and loading content

The kaempferol encapsulation efficiency and loading (%) of the synthesized nanoparticles were measured by UV/Vis spectrophotometer (PG Instruments, T60U UV-Visible, UK) at wavelength of 373 nm. After nanoparticles were centrifugated for 30 min at 12000 rpm, non-entrapped kaempferol concentration in recovered supernatant was determined. Supernatant recovered from nanoparticles without kaempferol was used as a blank. Possible kaempferol release was taken into consideration after every washings. Encapsulation efficiency (EE%), and loading content (LC%) were calculated by the following eqs. 1 and 2, respectively:

$$\mathrm{EE}(\%) = \left(\frac{\text{Actual amount of KAE encapsulated in NPs}}{\text{Initial amount of KAE used}}\right) \times 100 \qquad (1)$$

$$\mathrm{LC}(\%) = \left(\frac{\text{Weight of KAE in NPs}}{\text{Weight of NPs}}\right) \times 100 \qquad (2)$$

2.5. Nanoparticle morphology observation

Scanning Electron Microscopy (SEM) (Quanta FEG 250; FEI, North America) was used for the surface morphology of the kaempferol loaded chitosan nanoparticles. Before the examination, one drop of diluted nanoparticle suspension was mounted onto aluminium pin-type stubs (12 mm in diameter) with carbon tape. NPs were coated with gold to minimize the effect of heat during high-power magnification after drying procedure.

2.6. Evaluation of interactions of kaempferol with chitosan/TPP nanoparticle

The spectra of Fourier transform infrared spectroscopy (FT-IR) and ^{1}H nuclear magnetic resonance (^{1}H NMR) analyses were used to analyze molecular bonding formation between kaempferol and chitosan nanoparticles. The FT-IR spectra of pristine kaempferol and kaempferol loaded chitosan nanoparticles were recorded using Perkin Elmer Nicolet 520 spectrophotometer (Perkin Elmer, Boston, USA). The lyophilized samples were ground with spectroscopic grade potassium bromide (KBr) powder and then, pressed into 1 mm pellet for FTIR measurement in the range of 450-4000 cm^{-1} with 4 cm^{-1} resolution, using 16 scans. In addition, ^{1}H NMR spectra of samples was obtained from Bruker 2´300 NMR system (Bruker, Germany). For analysis, each sample (5 mg) was dissolved into 0.8 mL DMSO-d.

X-ray diffractometry (XRD) and differential scanning calorimetry (DSC) were used to determine the crystal polymorphism of free kaempferol and kaempferol loaded chitosan nanoparticles. The crystalline patterns of samples were obtained using the XRD (Panalytical, Empyrean) with Ni-filtered Cu Kα radiation. Measurement was performed at a voltage of 40 kV and 25 mA. The scanned angle was set from $2^{o} \leq 2\theta \leq 50^{o}$, and the scan rate was 1^{o} min^{-1}. The thermal transition properties of samples were recorded using Perkin Elmer DSC Q8000 calorimeter (Perkin Elmer Inc., Boston, USA). The thermal measurements were carried out (scanning rate:10 °C/min, temperature range:30-500 °C) under Ar purge (50 mL/min). All samples were analyzed and recorded in triplicate.

2.7. Measurement of antioxidant activities assays

2.7.1. Free radical scavenging capacity

The free radical scavenging activity of free kaempferol, empty chitosan nanoparticle and kaempferol loaded chitosan nanoparticle was measured by 1,1-diphenyl-2-picrylhydrazyl

(DPPH) assay according to literature with minor modifications Brand-Williams et al. [12] Briefly, 30 µL of sample solutions was added into 300 µL of DPPH ethanolic solution (0.2 m*M).* The reaction mixture was incubated in a shaker and left for 30 min at room temperature in the dark. The absorbance of the solutions was measured at 517 nm by UV/Vis spectrophotometer against a blank. The radical scavenging activity was calculated according to the following equation:

$$\text{Scavenging capacity (\%)} = (1 - \text{Abs}_{517\ \text{sample}} / \text{Abs}_{517\ \text{control}}) \times 100$$

2.7.2. Reducing power

The test ferric reducing antioxidant power (FRAP) of free kaempferol, empty chitosan nanoparticle and kaempferol loaded chitosan nanoparticle was performed according to the method discribed by Benzie and Strain [13] with some modifications. Initially, FRAP reagent (290 µL) was mixed with 10 µL of samples and incubated at 37 °C for 15 min. After incubation, the absorbance was determined at 593 nm using UV/Vis spectroscopy. FRAP reagent was freshly prepared by mixing (ratio 10:1:1) acetate buffer (pH 3.6, 300 mM/L), TPTZ (10 mM/L) in HCl (40 mM/L) and $FeCl_3$ (20 mM/L). The results were expressed as micromoles equivalent Fe^{2+} (Fe^{2+} µM).

2.8. In vitro release studies of kaempferol loaded chitosan nanoparticles

The in vitro release tests of kaempferol loaded chitosan nanoparticles were carried out in PBS containing DMSO (10%, v/v) release medium at 25 and 37 °C for 24 hours. Dialysis bags (pore size 2.5 nm, molecular weight cut off 12000-14000 Da, Himedia) containing nanoparticles suspension (10 mg/µL) were suspended in release media (30 mL), incubated at 25 and 37 °C and then, stirred at 100 rpm. At pre-determined time intervals, 3 mL of sample

was withdrawn and replaced with equal volume of the corresponding fresh medium. KAE concentration was assayed by using UV/Vis spectroscopy at 373 nm.

2.9. Stability studies of kaempferol loaded chitosan nanoparticles

The prepared nanoparticles were stored at 4 and 25 °C for 60 days in the dark. The kaempferol loaded chitosan nanoparticles properties were examined immediately post synthesis (T0) and after 10 days (T1), 20 days (T2) and 30 days (T3) of storage. The stability tests were performed by analysis of the particle size (nm), polydispersity index (PDI), zeta potential and antioxidant activity. All analysis was carried out in triplicate.

2.10. QS Inhibition against C. violaceum CV026

2.10.1. Disc diffusion assay

Disc diffusion assay was carried out to detect the anti-QS activity of nanoparticles. Briefly C6-HSL (0.25 μg/mL) was added to 100 mL of sterilized LB agar at an appropriate temperature and was then, gently mixed and poured into the petri plates. The overnight culture of *C. violaceum* CV026 was swabbed evenly onto a solidified agar surface. Sterile discs were loaded with appropriate volumes of nanoparticles at different storage periods (T0, T1, T2 and T3) and placed onto the agar plates, which were then incubated at 30 °C for 24 h. Halo formation on a purple background suggested that the nanoparticles exhibited anti-QS. Pure kaempferol in different storage time were used as control.

2.10.2. Quantitative determination of violacein inhibition

The flask incubation assay was carried out for the quantitative determination of violacein inhibition by nanoparticles. Inoculated LB broth supplemented with C6-HSL (5

μM) and nanoparticles at different storage time (T0, T1, T2 and T3) was incubated for 24 h at 30°C. Violacein extraction was carried out as described by Choo et al. [14]. Briefly, 1 mL of culture from each flask was centrifuged at 10,000 g for 5 min to precipitate violacein. The pellet was dissolved in 1 mL of dimethyl sulfoxide (DMSO) and vortexed robustly to solubilize the violacein completely. Above mixture was centrifuged again to remove the cells and was quantified at 585 nm using a microplate reader (Biotek, USA). The experiment was repeated for triplicate values and the percentage of inhibition was calculated by the formula as:

(control OD_{585} nm-testOD_{585} nm)/control OD_{585} nm X 100

3. Results and discussion

3.1. Particle size and zeta potential

In this study, chitosan/TPP nanoparticles were synthesized by ionic gelation method due to its easy and rapid characteristics. In this simple method, nanoparticles are formed spontaneously because of electrostatic interaction between positively charged amino group of chitosan and negatively charged TPP polyanions (Fig. 1). This technique can be controlled easily and therefore, size and surface charge properties of nanoparticles can be manipulated by changing parameters such as concentration, temperature and pH [15].

The hydrodynamic parameters and zeta potential index are essential parameters for evaluation of nanoparticles due to their influence on important properties such as encapsulation, release and stability of nanoparticles. In addition nanoparticles with different particle size and zeta potential have different inhibition activity against microorganism because of this size and surface charge are the important properties for nanoparticle

engineering systems used as antibiofilm agents [16]. Nanoparticles that have smaller size present high surface area which leads a high encapsulation efficiency and release ratio. However, smaller nanoparticles also have more aggregation risk during storage so the development of nanoparticles with a low polydispersity index (PDI) is important to achieve maximum stability [17-19]. There are several factors such as concentration and ratio of drug that affect particle size of nanoparticles. Therefore, in this study, the effects of different concentrations and mass ratio of kaempferol on particle size, polydispersity index and zeta potential of kaempferol loaded chitosan nanoparticles were investigated (Fig. 2). The results showed that the size of nanoparticles was greatly influenced by the concentration of kaempferol which was added into a constant amount of chitosan and TPP (Fig. 2A). It was observed that with increasing kaempferol concentrations in kaempferol loaded chitosan nanoparticle formulations lead increasing values of particle size and polydispersity index. The formulations containing 20, 30, 40, 60, 80, 100 µg of kaempferol/mL suspension presented low poly dispersity index (PDI≤0.25) within average sizes of 137.51, 139.27, 156.29, 168.72, 208.36, 272.92 nm, respectively. Results are in agreement with the works published by Souza et al. [17] and Pool et al. [20] that increased particle size observed with increased quercetin, a flavonoid, concentration in chitosan/lecithin and poly(lactic-co-glycolic acid) nanoparticles, respectively. Nanoparticles aggregation was observed after production when the nanoparticles were prepared with values higher than 80 µg kaempferol/mL. The presence of high concentration of kaempferol that may interfere with the nanoparticles by blocking behavior of repulsive forces because of decreasing of space between nanoparticles, thus leading to aggregation. Similar results were observed by Souza et al. [17] and Barbieri et al. [21] for chitosan nanoparticles with high loading of drug. Similar relationship was also observed with the mass ratio of kaempferol in which the effect on particle size was also very prominent (Fig.

2B). These relationships enable easy manipulation of nanoparticle size for application in variable fields.

Zeta potential has been suggested as a key factor for the antimicrobial effect of agents through the interaction with negatively charged microbial cell surface [22]. Kaempferol loaded chitosan nanoparticles had positive zeta-potential values from + 18.5 to + 38.1 mV at different concentration (Fig. 3A) and mass ratio (Fig. 3B) of kaempferol indicating that nanoparticles had positive surface charges as expected owing to excess positive charge of chitosan molecules after interaction with polyanions. From the results obtained that the values of particle positive charge increased linearly with the increasing concentration and mass ratio of kaempferol in chitosan nanoparticle formulation (Fig. 3). Similar results were reported that chitosan nanoparticles have positive surface charges at pH 4.5 with zeta-potential values around 30 mV [16, 23]

3.2. Kaempferol loading and encapsulation efficiency

The loading and encapsulation efficiency of kaempferol into chitosan/TPP nanoparticles presented higher values between 78-93 % for all used concentration (20, 30, 40, 60, 80, 100 µg of kaempferol/mL suspension) (Fig. 4). In addition, a larger amount of kaempferol was inserted into chitosan/TPP nanoparticles and only a small amount of kaempferol was lost in the aqueous phase during production of nanoparticles. The high encapsulation efficiencies can be releated to the presence of hydrophilic phenolic hydroxyl groups of kaempferol that can establish extensive hydrogen bonding which promote the interaction with chitosan. From the Fig. 4 it also observed that increasing the kaempferol concentration in the formulation resulted in improved kaempferol loading as expected [17].

3.3. Nanoparticle morphology

Surface properties and morphology of the nanoparticles play a crucial role in drug release kinetics. SEM measurement is an effective method to provide the surface morphology. The empty chitosan/TPP nanoparticles and kaempferol loaded chitosan/TPP nanoparticles are spherical in shape, and uniform formation. In addition, almost no particle aggregation occurred during the drying of the NPs (Fig. 5). From SEM image analysis, we may get an insight into the average particle size, which is about 168.62±10.2 nm for the empty chitosan/TPP nanoparticles (Fig. 5A) and and 192.27±13.6 nm for the kaempferol loaded chitosan/TPP nanoparticles (Fig. 5B), respectively. The results indicated that the loading of kaempferol leads to an increase of the particle size.

3.4. Spectroscopy evaluation

FTIR analyses were performed to investigate possible reactions between kaempferol and chitosan/TPP nanoparticle. The pure kaempferol spectrum (Fig. 6A-a) shows the characteristic absorption bands and typical molecular peaks of its structure: 3324 cm^{-1} (O─H stretch), 1661 cm^{-1} (C=O), 1604 cm^{-1} (C=C), 1378 cm^{-1} (C─OH), 1257 cm^{-1} (C─O─C). Furthermore, the kaempferol loaded chitosan/TPP nanoparticle spectrum showed that the C=O absorption band at 1661 cm^{-1} of kaempferol shifted to the 1653 cm^{-1} and the OH stretch of kaempferol completely disappeared at 3363 cm^{-1} (Fig. 6A-b). The results indicated that the intramolecular hydrogen bonding was formed between kaempferol and chitosan after nanoparticle engineering process [24]. The disappearance of characteristic peaks of flavonoid after encapsulation was also observed in chitosan nanoparticles by Zhang et al. [25].

The formation of hydrogen bonding can be also evaluated by the change in chemical shifts in NMR spectra. The ^{1}H NMR spectrum confirmed that kaempferol had a clear signal for strong intramolecular hydrogen bonds at 12.45 ppm and the characteristic peak of protons on aromatic groups ranging from 6 to 8 ppm (Fig. 6B-a). Furthermore, after encapsulation of

kaempferol by the nanoparticle engineering system, the intramoleculer hydrogen bonding of kaempferol completely disappeared and the peaks of aromatic protons were clearly shifted (Fig. 6B-b). This result demonstrated that the aromatic ring of kaempferol prominently presented intermolecular hydrogen bond with chitosan/TPP nanoparticles. Similar result was also obtained in kaempferol nanoparticles by Tzeng et al. [24].

3.5. DSC and XRD measurements

DSC was used to check any variation of crystalline properties of kaempferol due to the encapsulation into the chitosan nanoparticles. The DSC curve of kaempferol showed a endothermic single Tg peak around 286 °C which indicated that its crystalline structure (Fig. 7A-a). The presence of a single Tg confirms the complete homogeneous dispersion of kaempferol in the matrix of the carriers [24]. After the nanoparticle engineering, however, the kaempferol loaded chitosan/TPP nanoparticles had an amorphous pattern and the crystalline peaks seen in kaempferol disappeared (Fig. 7A-b). From the DSC results, it can be considered that as proof of inclusion of kaempferol into the chitosan nanoparticles in consequence of the thermal profile of kaempferol corresponding to its melting point disappeared.

In the X-ray diffractogram of pristine kaempferol had a highly crystalline structure and crystalline peak at a diffraction angle of 2θ =10.80°, 12.50°, 15.90°, 23.95°, 24.36°, 27.46° (Fig. 7B-a). However, the crystalline peaks of encapsulated kaempferol disappeared and after nanoparticle formation, an amorphous structure was observed (Fig. 7B-b). We suggested that nanoparticle engineering system could be formed a high-energy amorphous state. The absence of kaempferol peak may be due to the formation of kaempferol molecular dispersion in nanoparticle matrix. This result was in accordance with previously published data by Zhang et al. [25]. According to DSC and XRD results, kaempferol was transformed from crystalline

structure into amorphous structure due to intermolecular interactions with the nanocarriers matrix.

3.6. Antioxidant activity evaluation

Free radicals are generated from exogenous factors and agents and can easily initiate the peroxidation of membrane lipids. Kaempferol is a good antioxidant but several factors influence its antioxidant effect and limit its application, especially light and heat during preparation process. The DPPH free radical scavenging capacity assay was used to evaluate the ability of free-kaempferol and kaempferol loaded chitosan/TPP nanoparticles to donate protons. From the DPPH study, it was observed that the capacity of the phenolic group of kaempferol donated hydrogen in order to stabilize free radicals. Kaempferol loaded chitosan/TPP nanoparticles (scavenging activity %, 37 ± 2.5) were capable to reduce higher values of DPPH molecules compare to free kaempferol (scavenging activity %, 22 ± 1.8, data not shown). This result can be related with enhanced dissolution properties of kaempferol after encapsulation process. This phenomenon was also observed by Wu et al. [26] and Souza et al. [17] when encapsulating quercetin in nanoparticles based on polyvinyl alcohol and Eudragit® and in lecithin/chitosan nanoparticles, respectively. The reducing power of a compound can serve as a significant indicator of its antioxidant capacity. It was reported that the reducing power are generally associated with the presence of reductones, which have been shown to exert antioxidant action by breaking the free radical chain through donating a hydrogen atom [27]. The reducing power of free kaempferol and kaempferol loaded chitosan nanoparticles were examined. Kaempferol encapsulated chitosan nanoparticles (reducing power 1.8 ± 0.6 µM Fe^{2+}) were more effective in reducing Fe_3+ to Fe_2+ in comparison with free-kaempferol (reducing power 1 ± 0.2 µM Fe^{2+}, data not shown). The increased reducing

power of kaempferol after encapsulation again can be probably explained by an improvement in the dissolution properties of kaempferol in aqueous medium [24-26].

3.7. Release profiles

The release profiles of KAE from chitosan nanoparticles studies were carried out under different temperature (25 and 37 °C) conditions. The dissolution value of pristine kaempferol was less than 2% at two temperature conditions within 240 min. However, a slow release profile of the nanoparticles was obtained at 37 °C. KAE from chitosan nanoparticles was released more than 85% for the first 4 hours at 37 °C in buffer, no significant drug release was observed for the rest of the remaining time (Fig. 8). The release rates and efficiency of KAE from nanoparticles were strongly dependent on the proportion of chitosan and TPP. Specifically, the release efficiency of KAE was increased 43-fold as compared with pure KAE. According to previous studies [16,28,29], this may be related to small nanoparticles with enhanced surface area, resulting in a larger KAE concentration exposed to the releasing media.

3.8. Stability studies

The stability of pure kaempferol and kaempferol loaded chitosan nanoparticles at storage temperature 4 and 25 °C (room temperature) was assessed during a 30 day observation period by examining the changes in antioxidant activity (DPPH and FRAP) (Table 1). Pure KAE was showed fastly decreased antioxidant profiles at both temperature (4 and 25 °C) within immediately post preparation of solution (data not shown). However, insignificant differences were observed in the antioxidant activity of kaempferol loaded chitosan nanoparticles at 4 °C storage condition. At the end of 30 days of storage DPPH scavenging activity of antioxidant value reduced from 35 ± 2.7 % to 28 ± 2.5 % at 4 °C, while

antioxidant value of the same nanoparticle reduced from 34 ± 3.1 % to 7 ± 0.5 % at 25 °C . Similarly, FRAP reducing antioxidant power reduced from 1.8 ± 0.5 to 1.1 ± 0.4 µM Fe^{2+} at 4 °C, while antioxidant value of the same nanoparticle reduced from 1.6 ± 0.2 to 0.4 ± 0.09 µM Fe^{2+} at 25 °C. Thus, temperature was played a vital role in antioxidant activity of nanoparticle. As a result, the antioxidant activity of KAE demonstrated that KAE act as a good antioxidant but it is also easily oxidized by heat.. In addition, nanoparticles stored at room temperature showed linear reduction in antioxidant activities during the storage time. Storage at 4 °C reduced the rate of oxidation of the kaempferol loaded chitosan nanoparticles.

3.9. QSI bioassay

QS plays a vital role in biofilm formation and virulence factor production in several bacterial species. Consequently, compounds that interfere with the QS system attenuating the bacterial pathogenicity are termed as anti-QS compounds. Such compounds neither kill the bacteria nor stop their growth and are less expected to develop resistance towards antibiotics [30]. In this work, the anti-QS activity of kaempferol loaded chitosan nanoparticles and pure kaempferol at different storage time (T0, T1, T2 and T3) was evaluated using the reporter strain *C. violaceum CV026.* In the disc diffusion method, nanoparticles exhibited anti-QS activity against *C. violaceum CV026*, which was indicated by the loss of purple pigmentation. On the contrary, pure kaempferol was loss its QSI activity at T0 (data not shown). Tested nanoparticles showed the immediate zone of clearance within ranges at T0:24.63 mm, T1:18.52 mm, T2:14.22 mm and T3:10.36 mm which may be because of the bactericidal effect that is followed by the opaque, halo zone of clearance; this indicates the inhibition of violacein production (Fig. 9A). The results now obtained for the disc diffusion assay were more promising than the ones obtained by other researchers [31,32], for example, some phytochemicals, studied by Borges et al. [31] had not presented anti-QS activity with diameter

of violacein inhibition equal to 0 mm. In order to evaluate the extent of QSI, the extraction and quantification of violacein from *C. violaceum CV026* cultures in the presence of kaempferol loaded chitosan nanoparticles at different storage days (T0, T1, T2 and T3) were also performed. In quantitative analysis by the flask incubation assay, nanoparticles at all tested storage time significantly reduced violacein production in tests when compared with pure kaempferol. Our results are true to the fact that the potential advantages of nanoparticles like low turbidity, high stability and solubility over conventional ones make them excellent systems [33,34]. Nanoparticles exhibited 76.21% inhibition at T0 as highest and at T3 inhibited 33.92% of violacein production when compared to that of control (Fig. 9B). In this study kaempferol loaded chitosan nanoparticle formulations inhibited violacein production up to 76% which indicates that kaempferol encapsulated into chitosan nanoparticles can act as strong and longtime stable quorum quenchers than the corresponding pure kaempferol. Present study illustrated that, the encapsulated kaempferol into chitosan nanoparticles presents as a class of compounds with promising sustainable QSI activity.

4. Conclusions

We have demonstrated the QS inhibitory stability of encapsulated kaempferol into chitosan against the reporter strain *C. Violaceum CV026.* Since quorum sensing plays a major role in food spoilage, biofilm formation, and food-related pathogenesis, the present investigation may help to point out the potential of kaempferol loaded chitosan nanoparticles as possible QS inhibitors. The obtained results exhibited that the formulated encapsulated kaempferol into chitosan nanoparticles at different storage time periods effectively regulated bacterial phenotypes like violacein pigmentation and biofilm formation when compared with pure kaempferol. At the end of the storage time period nanoparticles exhibited pronounced activity. Hence, by this study, we lay a solid foundation for the use of kaempferol loaded chitosan nanoparticles as a suitable alternative over conventional antimicrobials. Formulated

nanoparticles were tested for stability proves its candidature for field utilization. Novel kaempferol loaded chitosan nanoparticles are ideal for treatment and/or for surface decontamination of bacterial infections with the aid of QS-based antibacterial drugs.

Acknowledgements

We would like to thank Ayhan Şahenk Foundation for their support for laboratories of Ayhan Şahenk Agricultural Sciences and Technologies Faculty. We are also thankful for Prof. Dr. Robert Mclean from Texas State University, San Marcos for supplying us *Chromobacterium violaceum CV026*. This work was supported by the research program of the Hacettepe University (014 D12 101 005-820) and and The Scientific and Technological Research Council of Turkey (TUBITAK) with PhD Scholarship (2211/C).

References

[1] C.M. Waters, B.L. Bassler, Annu. Rev. Cell. Dev. Biol. 2005 (2005) 319–46.

[2] R.B. Raffa, J.R. Iannuzzo, D.R. Levine, K.K. Saeid, R.C. Schwartz, N.T. Sucic, O.D. Terleckyj, J.M. Young, J. Pharmacol. Exp. Ther. 312 (2005) 417-23.

[3] S. Gibot, Crit. Care. Med. 32 (2004) 1223-4.

[4] A.Y.B. Teoh, M. Hui, K.Y. Ngo, J. Wong, K.F. Lee, P.B.S. Lai, Hong Kong Med. J. 2006 (12) 228–231.

[5] R.S. Blosser, K.M. Gray, J. Microbiol. Methods. 2000 (40) 47–55.

[6] K.H. McClean, M.K. Winson, L. Fish, A. Taylor, S.R. Chhabra, M. Camara, M. Daykin, J.H. Lamb, S. Swift, B.W. Bycroft, Microbiology. 1997 (143) 3703–3711.

[7] A. Gupta, C.D. Kaur, S. Saraf, S. Saraf, Artif. Cells Nanomed. Biotechnol. 27 (2015) 1-11.

[8] K.S. Yadav, K.K. Sawant, AAPS. 11 (2010) 1456-65.

[9] A.M. Chuah, T. Kuroiwa, I. Kobayashi, M. Nakajima, Food Hydrocoll. 23 (2009) 600-610.

[10] P. Calvo, C. Remuñán-López, J.L. Vila-Jato, M.J. Alonso, J. Appl. Polym. Sci. 63 (1997) 125-132.

[11] W. Fan, W. Yan, Z. Xu, H. Ni, Colloid. Surface. B. 90 (2012) 21-7.

[12] W. Brand-Williams, M.E. Cuvelier, C. Berset, Food Sci. Technol. 28 (1995) 25-30.

[13] I.F.F. Benzie, J.J. Strain, Anal. Biochem. 239 (1996) 70-76.

[14] J.H. Choo, Y. Rukayadi, J.K. Hwang, Lett. Appl. Microbiol. 42 (2006) 637-41.

[15] Q. Gan, T. Wang, C. Cochrane, P. McCarron, Colloid. Surface. B. 44 (2005) 65-73.

[16] L.Y. Ing, N.M. Zin, A. Sarwar, H. Katas, Int. J. Biomater. 2012 (2012) 9.

[17] M.P. Souza, A.F. Vaz, M.T.S. Correia, M.A. Cerqueira, A.A. Vicente, M.G. Carneiro-da-Cunha, Food Bioprocess. Tech. 7 (2014) 1149-1159.

[18] A. Bayata, F.A. Dorkoosha, A.R. Dehpourc, L. Moezic, B. Larijanid, H.E. Jungingere, M. Rafiee-Tehrani, Int. J. Pharm. 2008 (356) 259–266.

[19] K. Yoncheva, B. Tzankov, M. Popova,V. Petrova, N. Lambov, J. Dısper. Scı. Technol. 2016 (37) 113-118.

[20] H. Pool, D. Quintanar, J.D. Figueroa, C.M. Mano, J.E.H. Bechara, L.A. Godinez, S. Mendoza, J. Nanomater. 2012 (2012) 12.

[21] S. Barbieri, F. Sonvico, C. Como, G. Colombo, F. Zani, F. Buttini, R. Bettini, A. Rossi, P. Colombo, J. Control. Release. 167 (2013) 276-283.

[22] L.C. Chen, S.K. Kung, H.H. Chen, S.B. Lin, Carbohydr. Polym. 82 (2010) 913-919.

[23] H.-K. Ha, J.W. Kim, M.-R. Lee, W.-J. Lee, Food Res. Int. 52 (2013) 82-90.

[24] C.W. Tzeng, F.L. Yen, T.H. Wu, H.H. Ko, C.W. Lee, W.S. Tzeng, C.C. Lin, J. Agric. Food Chem. 59 (2011) 5073-80.

[25] Y. Zhang, Y. Yang, K. Tang, X. Hu, G. Zou, J. Appl. Polym. Sci. 107 (2008) 891-897.

[26] T.-H. Wu, F.-L. Yen, L.-T. Lin, T.-R. Tsai, C.-C. Lin, T.- M. Chamd, Int. J. Pharm. 346 (2008) 160-168.

[27] M. Ozgen, R.N. Reese, Jr.A.Z Tulio, J.C. Scheerens, A.R. Miller, J. Agric. Food Chem. 54 (2006) 1151-1157.

[28] L. Gao, D. Zhang, M. Chen, C. Duan, W. Dai, L. Jia, W. Zhao, Int. J. Pharm. 355 (2008) 321-7.

[29] Q. Tan, W. Liu, C. Guo, G. Zhai, Int. J. Nanomedicine. 6 (2011) 1621-30.

[30] S.V.P. Abraham, A. Palani., B.R. Ramaswamy, K.P. Shunmugiah, V.R. Arumugam, Arch. Med. Res. 42 (2011) 658-668.

[31] A. Borges, S. Serra, A.A. Cristina, M.J. Saavedra, A. Salgado, M. Simões, Journal of Bioadhesion and Biofilm Research, 30 (2014) 183-95.

[32] B.N. Singh, B.R. Singh, R.L. Singh, D. Prakash, B.K. Sarma, H.B. Singh, Food Chem. Toxicol. 47 (2009) 778-86.

[33] H.D. Silva, M.A. Cerqueira, A.A. Vicente, Food Bıoprocess. Tech. 5 (2012) 854-867.

[34] D.J. McClements, J. Rao, Crit. Rev. Food Sci. Nutr. 51 (2011) 285-330.

Figure captions

Fig. 1. Schematic illustration of kaempferol encapsulated chitosan nanoparticles.

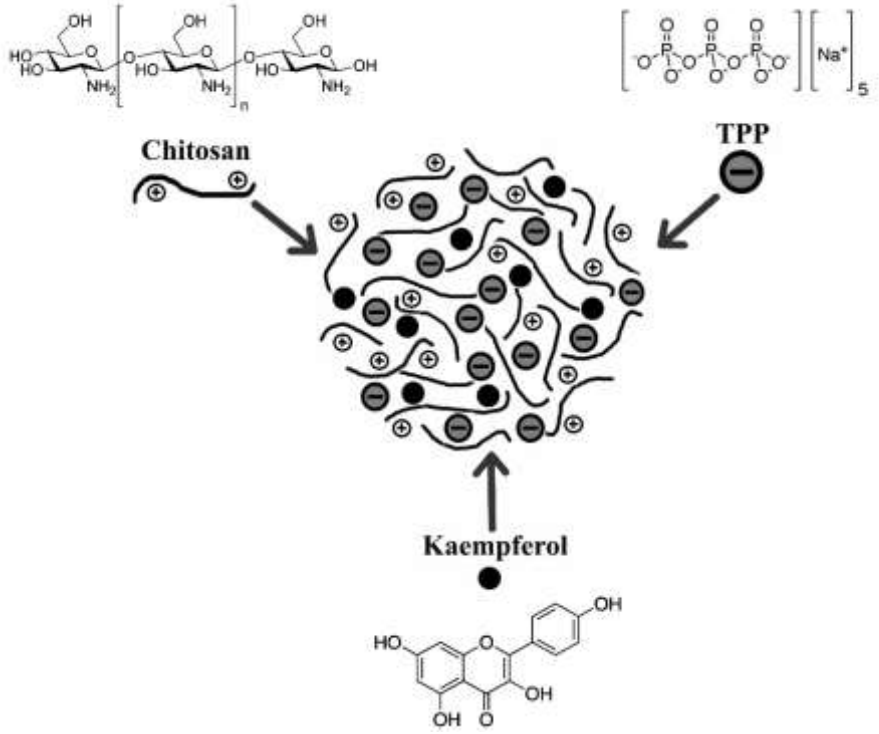

Fig. 2. Influence of encapsulated kaempferol (A) concentration (B) ratio to chitosan/TPP ratio on the average size (*black squares*) and polydispersity index (*grey bars*) of chitosan nanoparticles.

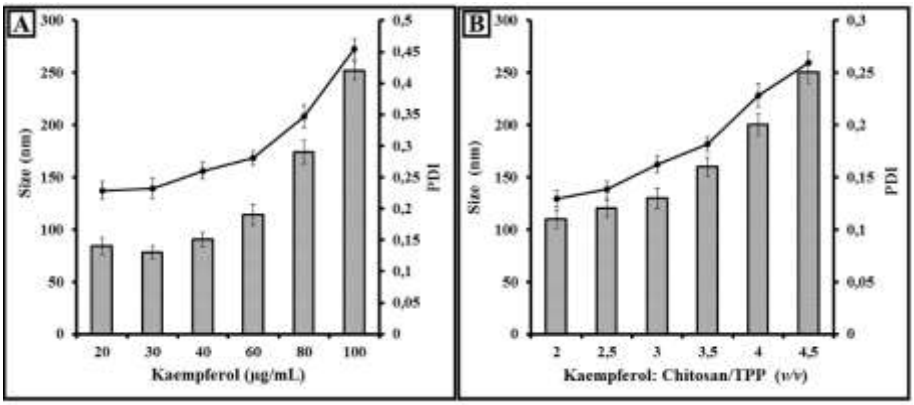

Fig. 3. Influence of kaempferol (A) concentration (µg/mL) (B) ratio (mL/mL) to chitosan/TPP ratio on the surface charge of chitosan nanoparticles.

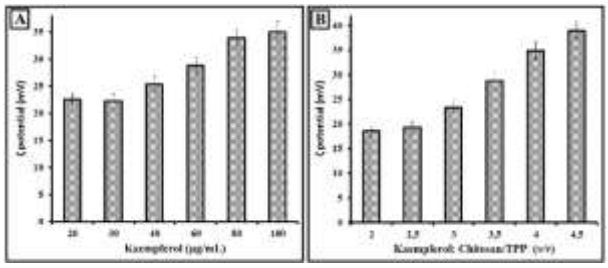

Fig. 4. Loading content (*black squares*) and encapsulation efficiency (*grey bars*) of kaempferol into chitosan nanoparticles.

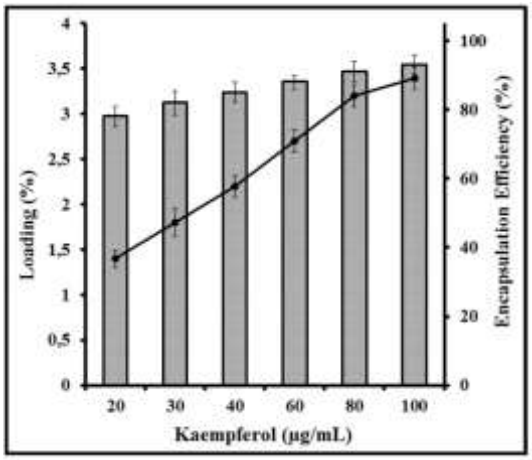

Fig. 5. Scanning electron microscopy images. Morphology and dispersivity of (A) chitosan nanoparticles and (B) kaempferol loaded chitosan nanoparticles.

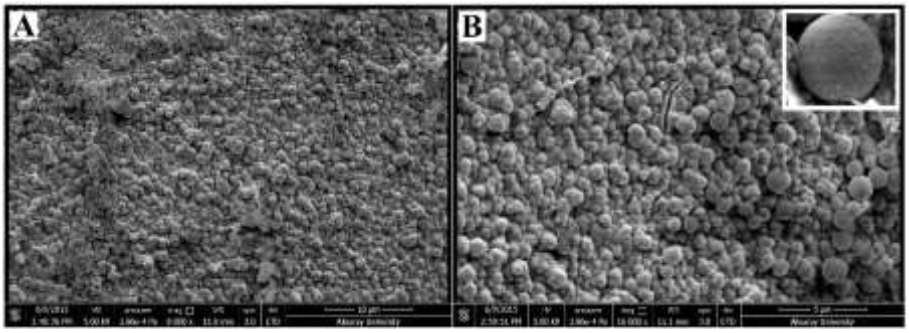

Fig. 6. (A) FTIR spectra and (B) ^{1}H NMR spectra of (a) pure kaempferol and (b) kaempferol loaded chitosan nanoparticles.

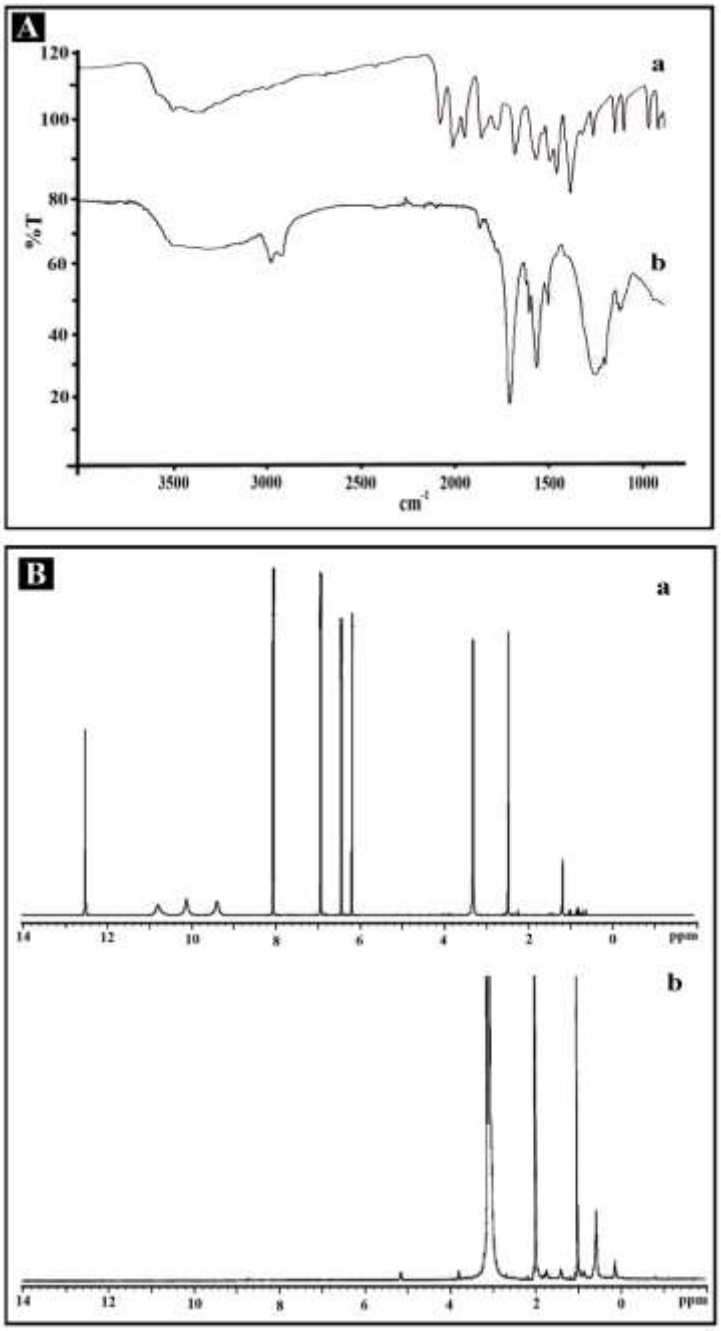

Fig. 7. (A) DSC patterns of (a) pure kaempferol and (b) kaempferol loaded chitosan nanoparticles, (B) XRD patterns of (a) pure kaempferol, (b) empty chitosan nanoparticles and (c) kaempferol loaded chitosan nanoparticles.

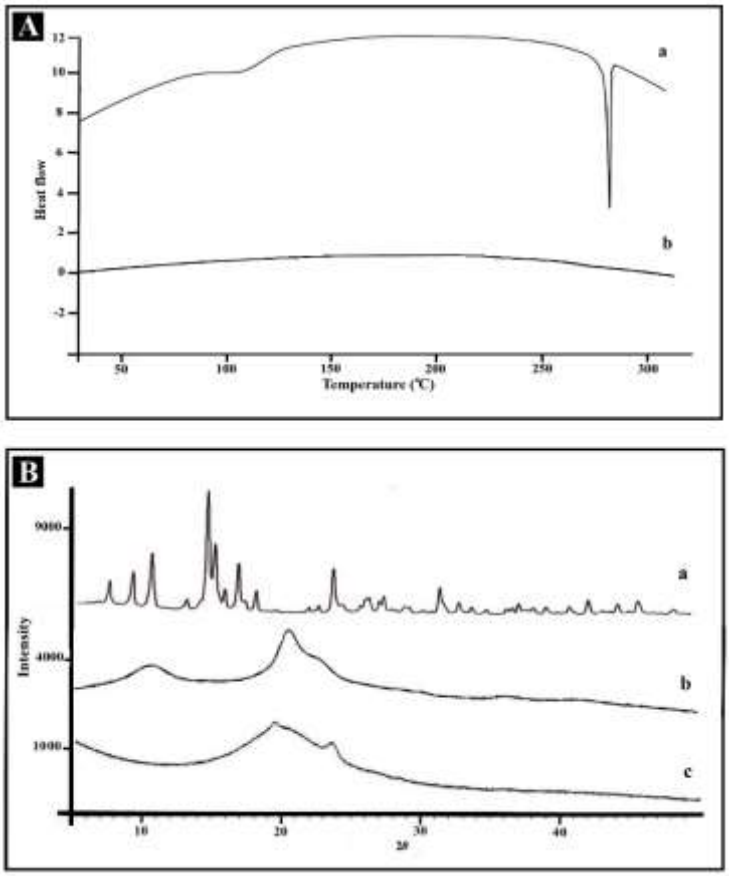

Fig. 8. *In vitro* release profiles of KAE from chitosan nanoparticles at 37 ºC and at 25 ºC conditions.

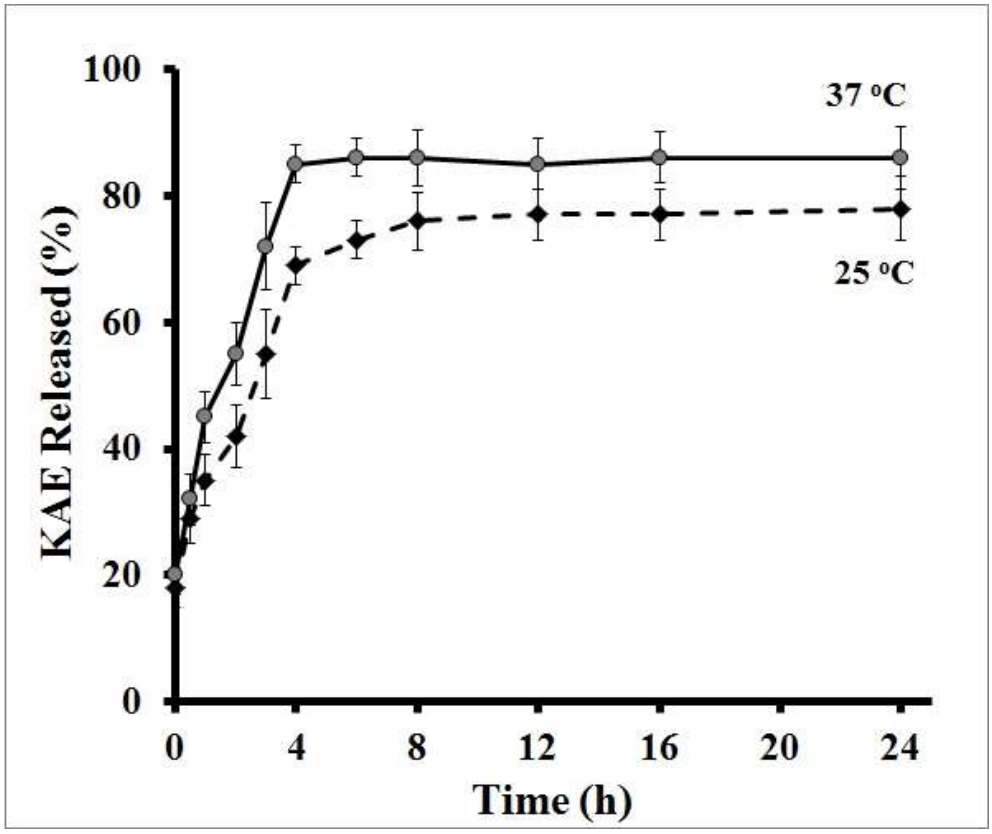

Fig. 9. (A) Plate diffusion assay for the quorum sensing inhibition (B) quantitative determination of violacein inhibition by kaempferol loaded chitosan nanoparticles at different storage time (T0: immediately post synthesis, T1: 10th day, T2:20th day and T3:30th day) against reporter strain *C. violaceum* CV026.

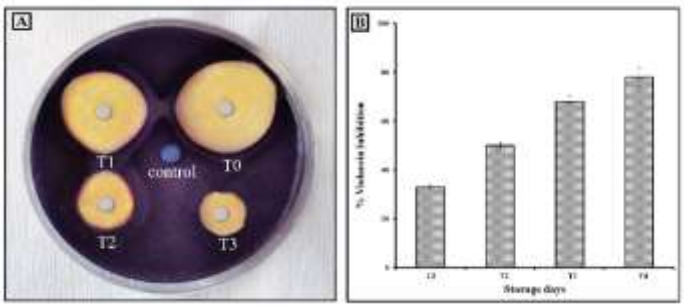

Table 1. Changes in antioxidant activity of kaempferol loaded chitosan nanoparticles depending on storage time and temperature.[a] The kaempferol loaded chitosan nanoparticles properties were examined immediately post synthesis (T0) and after 10 days (T1), 20 days (T2) and 30 days (T3) of storage.

	T0		**T1**		**T2**		**T3**	
	4 °C	**25 °C**	**4 °C**	**25 °C**	**4 °C**	**25 °C**	**4 °C**	**25 °C**
DPPH Scavenging capacity (%)	35 ± 2.7	34 ± 3.1	32 ± 2.2	21 ± 1.9	30 ± 2.4	16 ± 1.1	28 ± 2.5	7 ± 0.5
FRAP Reducing power (µM Fe^{2+})	1.8 ± 0.5	1.6 ± 0.2	1.5 ± 0.4	1.0 ± 0.2	1.2 ± 0.3	0.7 ± 0.1	1.1 ± 0.4	0.4 ± 0.09

[a] All determinations were performed in triplicate and values are expressed as mean ±S.D., n=3